

Cellulose-based fibres from liquid crystalline solutions: 5. Processing and morphology of CAB blends with lignin

Vipul Davé and Wolfgang G. Glasser*

Department of Wood Science and Forest Products, Biobased Materials Center, and Polymer Materials and Interfaces Laboratory, Virginia Tech, Blacksburg, VA 24061, USA

(Received 3 July 1993; revised 25 July 1996)

Continuous fibers from blends of cellulose acetate butyrate (CAB) with lignin (L) were spun from liquid crystalline solution. Morphological investigations suggest that CAB and L form blends with considerable phase mixing. The porosity of the surface structure of CAB/L fibres increased with increasing L content. The mechanical properties of the L-containing fibres increased with phase mixing of CAB and L molecules in the fibre matrix. This study shows that phase mixing can be enhanced by coagulation during wet spinning.
 © 1997 Elsevier Science Ltd.

(Keywords: cellulose esters; lignin; polymer blends; fibre spinning; liquid crystalline; phase mixing; mechanical properties)

INTRODUCTION

Blending polymers is a simple way of modifying properties of materials for particular applications at reasonable price/performance ratios. Non-mesomorphic polymer blends have been extensively studied^{1–3}, and incompatibility is observed unless specific interactions exist between different constituents.

When one component is liquid crystalline, the polymer blend may produce ultrahigh modulus composites^{4–8}. In the case of mixtures of rigid-rod-like components and random coils in a solvent, the latter component is predicted to be virtually excluded from the liquid crystalline phase⁹. This is due to an entropy effect related to the interference of the random coils with the orientation of the rod-like molecules. Aharoni's experiment on the ternary system of tetrachloroethane/polyisocyanate (POIC)/polystyrene supported this prediction as polystyrene was not present in detectable quantities in the anisotropic POIC phase¹⁰. Bianchi *et al.*¹¹ also showed that the flexible polymer X-500 (polyterephthalamide of *p*-aminobenzhydrazide) was not observed in the anisotropic phase of poly(*p*-benzamide) (PBA) in a ternary system of X-500/PBA/dimethylacetamide. Also, two mesogenic polymers, cellulose acetate (CA) and hydroxypropyl cellulose (HPC), were found not to be compatible in isotropic and anisotropic dimethylacetamide solutions, giving rise to three coexisting phases¹². Similar incompatibility was observed between anisotropic solutions of HPC and ethyl cellulose (EC) in acetic acid¹³. However, the bulk morphology of these blend systems has not yet been investigated.

In the cell wall of wood, the carbohydrate component is closely associated with lignin (L)—a polymer showing network-like behaviour. L is a major component of the structural matrix, imparting strength and rigidity to the cell wall. The interaction of L and cellulose (C) in this

natural composite is not well understood. Blend studies on melt-extruded and solvent-cast films of HPC and L have shown the presence of secondary interactions between the two components. This has been represented as a partially miscible system¹⁴. Although blends of L with EC and CAB were determined to be immiscible by thermal analysis¹⁵, recent studies on solvent-cast blended films of CAB from liquid crystalline solutions revealed an enhanced cholesteric structure of the CAB phase¹⁶. This was shown to be caused by micron-size L particles which may have provided nucleating surfaces for the CAB molecules¹⁶.

The processing and morphological features of fibres from liquid crystalline solutions of CAB¹⁷, C¹⁸, and cellulose hexanoate¹⁸ have been the subject of prior publications. The effect of lithium chloride on CAB fibre properties was studied by creep tests under cyclic moisture conditions¹⁹. The objective of the present study was to investigate the effect of L on the properties of CAB solutions, and to evaluate the blend morphology of the fibres spun from these solutions.

EXPERIMENTAL

Materials

Cellulose acetate butyrate (CAB 500-5) was obtained from Eastman Kodak, Kingsport, TN. The degree of substitution (DS) by acetyl (DS_{ac}) and butyryl (DS_{bu}) groups was 0.29 and 2.57, respectively. DS_{OH}, determined by difference, was 0.14.

Unmodified organosolv lignin was supplied by Aldrich (Cat. No. 37, 101-7). Reagent-grade dimethylacetamide (DMAc) and lithium chloride (LiCl) were used as received.

Methods

Preparation of blended solutions. Individual component solutions of dried CAB and L were prepared in

* To whom correspondence should be addressed

DMAc. These were mechanically mixed for 12 h at ambient temperature. The total solids content of all solutions was kept constant at 40% (w/w), and the L content varied between 4 and 20% (w/w) of organic solutes. (CAB 500-5 had previously been shown by rheological investigations to form liquid crystalline solutions in DMAc above 35% (w/w) concentration²⁰.)

Viscosity measurements. A Rheometrics Mechanical Spectrometer (RMS 800) (parallel disc geometry) was used to determine the rheological properties of the solutions. The dynamic mechanical properties were measured at 26°C using a strain amplitude of 25% of the value at which the respective solution showed viscoelasticity. All solutions exhibited viscoelastic behaviour. The frequency ranged from 0.1 to 100 rad s⁻¹.

Polarized optical microscopy. Polarized optical microscopy was performed using a Zeiss Axioplan microscope. Small portions of the solutions were placed between microscope slide and cover slip, and these were inspected for birefringence between the crossed polarizers of the microscope at room temperature.

Fibre spinning. Continuous blended fibres were spun by a dry jet/wet spinning method from a capillary with a diameter of 300 µm, as described previously¹⁷. The flow rate of the solutions varied between 1 and 3 cm³ min⁻¹. The fibres were taken up on the spools at speeds varying from 11 to 25 m min⁻¹. The air gap was about 1 inch. Water was used as coagulant at about 30°C. The fibre-wound spools were immersed in beakers containing water that was periodically exchanged for fresh water for 8 h before they were allowed to air-dry for ca. 8–10 h. Care was taken to ensure that all residual solvent was removed from the fibre spools. All fibre tests were performed on fibres section from several locations of the spools; test results represent mean average values of at least 6–10 measurements; and results did not reveal any variability with location on the spool. This ensures that solvent exchange was constant and complete. The fibres were vacuum-dried for 24 h at 50°C. No post-spinning treatments were performed.

Fibre diameter. The fibre diameter *D* was determined using a Nikon UM-2 Measurescope equipped with a Quadra-Chek III attachment. The diameter was generally constant along an extended length of the fibre. The reported value is an average of 3–4 measurements along the fibre length.

Mechanical properties. The mechanical properties of the fibres were determined on an Instron 1130 test instrument following the procedure of ASTM standard D3822. Tests were conducted at room temperature and 67% relative humidity with 1 inch gauge length at a strain rate of 0.2 inch min⁻¹. Single blended fibres were used during testing. The linear density of the fibres varied between 94 and 270 denier for the blends. The values of initial modulus (*E*), breaking tenacity (σ_b), breaking toughness (*BT*), and elongation at break (ϵ_b) represent averages of 6–10 measurements.

Thermal analysis. Thermal analysis data of the CAB/L blended fibres were collected using a DuPont 912 d.s.c. at a heating rate of 10°C min⁻¹ under nitrogen,

between 30 and 280°C. After the first run, the samples were quenched to 30°C and re-heated to 280°C to observe the glass transition temperature. During sample preparation, the fibres were cut into small pieces. These were placed into d.s.c. pans which were sealed. Sample weight varied between 3 and 6 mg (it was difficult to fill the pans completely with short, light-weight fibres).

Scanning electron microscopy (SEM). The fibres were observed on a JEOL JSM-35C scanning electron microscope with an accelerating voltage of 15 kV. Fracture surfaces were formed in liquid nitrogen. The fibres were mounted on aluminum specimen mounts (EMSL) at an angle of 45°. The fibres were coated at the bottom by Ladd silver conducting paint and were then sputter coated by pure gold for 1 min (thickness ~9 nm) using an SPI sputter coater.

Transmission electron microscopy (TEM). Blended fibres were embedded in Poly/Bed 812 (Polysciences, Inc.) and cured at 60°C for 48 h in flat molds. Sections (80–90 nm thick) were cut cross-wise and length-wise from the embedded fibres with a diamond knife mounted on a Reichert Ultracut E microtome. All the sections were mounted on copper grids. Staining was carried out for 30 min by exposing some of the copper grids to vapours of a 0.5% stabilized aqueous solution of ruthenium tetroxide (RuO₄) (Polysciences, Inc.) in a small thin layer chromatography jar. The copper grids with the CAB/L sections were observed on a JEOL JEM-100CX-II electron microscope operated at an accelerating voltage of 80 kV.

RESULTS AND DISCUSSION

The molecular characteristics of CAB and L (Table 1) reveal that L is a relatively small molecule in comparison to CAB, and that its MHS constant, *a*, represents random coil conformation.

Dynamic viscoelastic properties

The relationship between dynamic shear viscosity and concentration of blended solutions of CAB with varying L content, at different frequencies, reveals decreasing viscosity with increasing L content (Figure 1a). In these solutions, CAB is gradually replaced by increasing amounts of L to maintain a total solids content of 40% (w/w). All solutions exhibit shear thinning behaviour. The corresponding relationship with dynamic elastic modulus (*G'*) (Figure 1b) indicates that *G'* increases with increasing frequency. This behaviour is expected for viscoelastic materials. The gradual drop in *G'* with increasing L content suggests that the amount of energy stored and dissipated per cycle of deformation

Table 1 Chemical and molecular characteristics of cellulose acetate butyrate and lignin

	Cellulose acetate butyrate	Organosolv lignin
$\langle M_n \rangle (\times 10^3)$	53	0.8
$\langle M_w \rangle (\times 10^3)$	125	3.5
DP_n	150	4
MHS constant, <i>a</i>	0.95	0.18
Intrinsic viscosity (dl g ⁻¹)	1.51	0.051

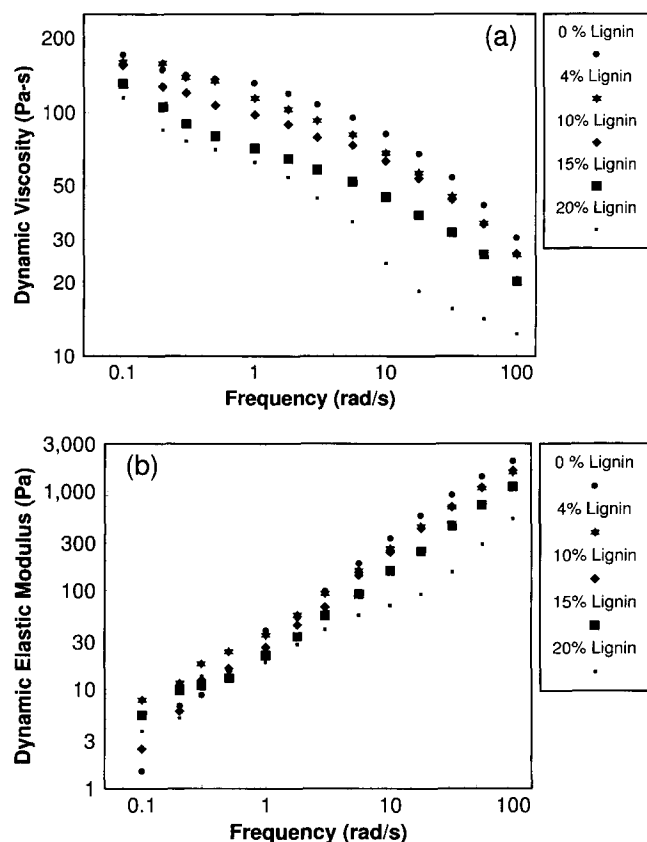


Figure 1 (a) Dynamic viscosity and (b) dynamic elastic modulus vs frequency of CAB/L solutions

decreases with increasing L content. It should be noted that the values for solutions containing lignin are higher than those of the control at low frequencies ($< 1 \text{ rad s}^{-1}$) (Figure 1b).

Polarized optical microscopy

The polarized optical micrographs of CAB solutions containing 0, 4, 15 and 20% (w/w) L, respectively, reveal that the anisotropic solution at 40% (w/w) concentration without L (Figure 2a) maintains the liquid crystalline order in the presence of increasing L (Figures 2b–d). It appears that the solution containing 20% L is more birefringent than the solution with 4 and 15% L. This is consistent with Flory's theory⁹; i.e., the presence of a flexible polymer will lower the critical concentration of the rigid or semi-rigid polymer. Similar observations were reported for ternary solutions of cellulose triacetate/poly(methyl methacrylate)/trifluoroacetic acid–methylene chloride²¹. Without a ternary phase diagram, these observations by optical microscopy remain purely qualitative. However, TEMs of the films prepared from the CAB/L solutions have shown direct evidence of cholesteric morphology¹⁶.

Processing and mechanical properties

Spinning conditions and mechanical properties of fibres from blends of L with CAB are summarized in Table 2. The take-up velocity, V_1 , varied between 11 and 21 m min^{-1} . The shear rate during spinning was about 6220 s^{-1} in relation to V_0 . A draw ratio of less than 1 is due to die swell. Liquid crystallinity and low viscosity improved the spinnability of CAB/L solutions. The term 'spinnability' is hereby used to describe the ability of

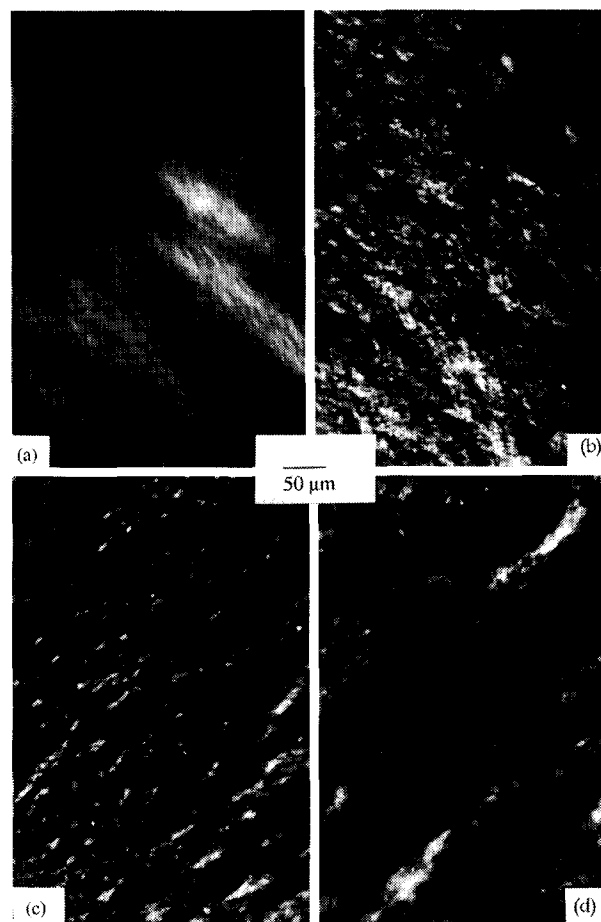


Figure 2 Polarized optical micrographs of CAB/L solutions with varying lignin content: (a) 0% L (w/w); (b) 4% L (w/w); (c) 15% L (w/w); and (d) 20% L (w/w)

Table 2 Spinning conditions and mechanical properties of fibres from blends of cellulose acetate butyrate and lignin^a

Lignin content (wt%)	V_1^b (m min^{-1})	Draw ratio ^c	D (μm)	E^d (g d^{-1})	σ_b (g d^{-1})	ϵ_b (%)	BT (g d^{-1})
0	11	0.80	214	10.5	0.4	16.0	0.05
0	15	1.07	156	12.2	0.6	21.3	0.08
0	21	1.50	155	22.6	0.8	11.0	0.06
4	11	0.80	241	18.4	0.8	8.6	0.04
4	15	1.07	207	18.2	0.8	9.7	0.05
4	21	1.50	158	18.5	0.9	12.6	0.07
10	11	0.80	304	17.0	0.7	11.7	0.06
10	15	1.07	247	18.4	0.8	11.4	0.06
10	21	1.50	200	16.9	0.7	14.8	0.07
15	11	0.80	208	14.3	0.7	13.8	0.06
15	15	1.07	196	15.2	0.7	14.6	0.07
15	21	1.50	167	17.5	0.8	15.4	0.08
20	11	0.26	190	20.6	0.6	9.5	0.05
20	15	0.35	167	20.8	0.7	12.0	0.06
20	21	0.50	161	16.6	0.6	10.5	0.04

^a The total solids content in all the solutions was maintained at a constant value of 40% (w/w) and lignin content varied from 4 to 20% (w/w). Each experimental test represents the mean average value of at least 6 to 10 measurements

^b V_1 represents the velocity of the take-up roller. V_0 represents the velocity of the spinning solution in the spinnerette hole. This was kept constant at 14 m min^{-1} except for the fibres with 20 (wt%) lignin content where V_0 was 42.5 m min^{-1}

^c Draw ratio = V_1/V_0

^d $1 \text{ GPa} \approx 8.5 \text{ g d}^{-1}$

the solutions to form fibres without experiencing any instability, such as filament breaks or drop formation. The viscosity of liquid crystalline solutions is lower than those of the corresponding isotropic solutions, so fibre formation is enhanced while spinning. However, if the viscosity of the solutions is very low then fibre-forming ability is reduced because of spinning instabilities. Such problems were experienced during spinning from solutions containing high amounts of lignin (i.e., >20% w/w).

Modulus and tenacity of fibres from blends of L and CAB varied with L content (Table 2). An almost 80% increase in fibre modulus is recorded with only 4% L content, and this remains approximately constant at higher L contents. The increase in liquid crystalline order with increased lignin content may possibly be responsible for the rise in fibre modulus. The failure to exhibit additional changes in fibre properties with increasing L contents is surprising. L has been shown to be a 'modulus-builder' in polymer blends¹⁴. Take-up speed does not have any influence on the modulus, although the value decreases somewhat at 21 m min⁻¹ for the fibres with L. The rise in tenacity follows the modulus data.

Thermal analysis

Figures 3a-f are the d.s.c. traces (first run) of CAB powder and fibres from anisotropic solutions of CAB/L.

CAB powder had a melting transition at 162°C, which represents the melting of a butyrate-rich copolymer¹⁷. CAB fibres without (Figure 3b) and with lignin (Figures 3c-d) displayed an extremely sharp melting transition which showed that the crystals were very well organized even in the presence of lignin. It is, however, observed that the melting transition became less sharp for the fibres with 15 and 20% L (Figures 3e and f).

Table 3 summarizes the thermal transitions of the CAB/L fibres. The melting point of the fibres declined with increasing L content. The heats of fusion of the blends suggest that the presence of an amorphous L component does not reduce the amount of crystallinity of the CAB component in the fibres. A glass transition temperature was not observed during the first d.s.c. scan, and the reported T_g values are from the second scan of the melted fibres. The melt-quenched fibres were completely glassy as no melting transitions were observed. Single glass transition temperatures and similar solubility parameters of 11.1 and 11.6 (cal cm⁻³) for L and CAB¹⁵, respectively, serve as evidence for miscibility.

These observations suggest that L and CAB are miscible at L contents of $\leq 20\%$ in the fibre structure.

Scanning electron microscopy (SEM)

The scanning electron micrographs of the surfaces of

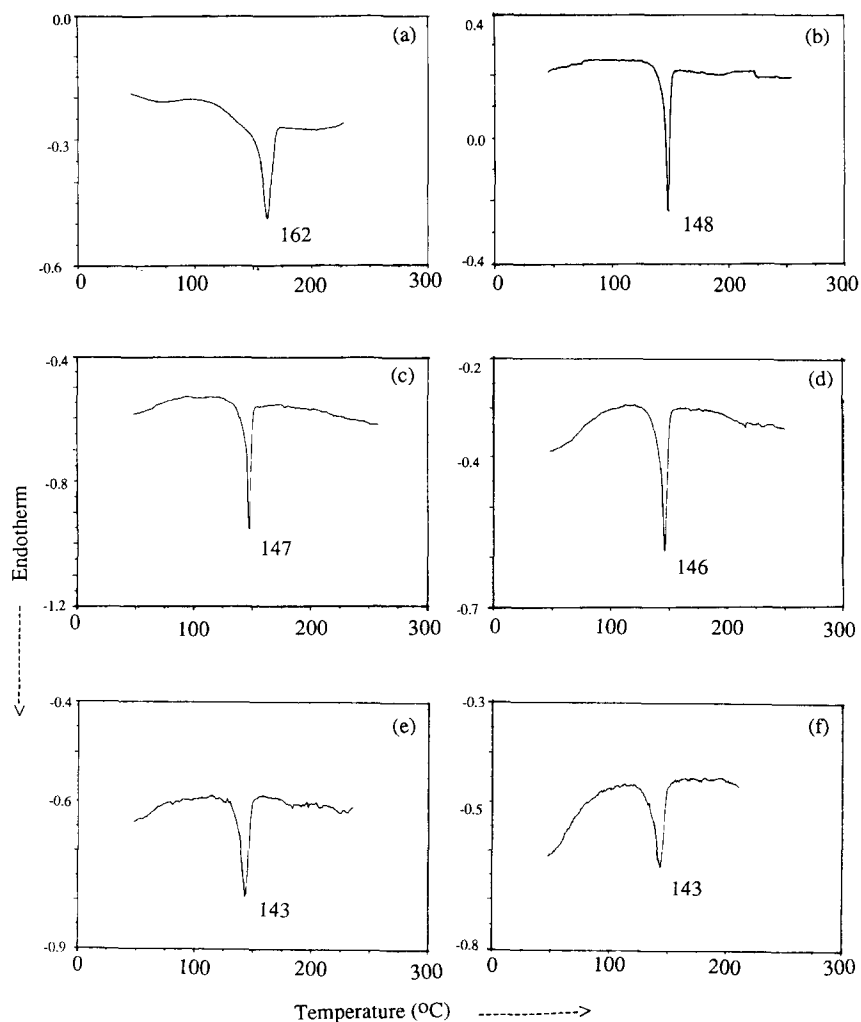


Figure 3 D.s.c. traces (first run) of CAB/L fibres spun at 11 m min⁻¹ with varying lignin content: (a) CAB powder; (b) 0% L (w/w); (c) 4% L (w/w); (d) 10% L (w/w); (e) 15% L (w/w); (f) 20% L (w/w)

Table 3 Glass transition temperature (T_g) and melting parameters (T_m , ΔH) of fibres from blends of cellulose acetate butyrate and lignin, determined by d.s.c

Lignin content (wt%)	V_1 (m min^{-1})	T_g ($^{\circ}\text{C}$)	T_m ($^{\circ}\text{C}$)	H (J g^{-1}) ^a
0 (CAB powder)	—	97	162	13.7 (13.7)
0	11.0	103	148	13.2 (13.2)
0	15.0	102	147	12.9 (12.9)
0	21.0	102	147	13.1 (13.1)
4	11.0	104	147	12.8 (13.3)
4	15.0	106	147	12.6 (13.2)
4	21.0	105	146	12.9 (13.5)
10	11.0	102	146	12.4 (13.8)
10	15.0	104	146	12.7 (14.2)
10	21.0	104	146	12.4 (13.8)
15	11.0	99	143	9.5 (11.2)
15	15.0	105	143	11.3 (13.3)
15	21.0	97	143	9.9 (11.7)
20	11.0	100	143	10.9 (13.6)
20	15.0	98	143	11.5 (14.4)
20	21.0	97	143	11.3 (14.1)
100 (lignin powder)	—	100	—	—

^a Values in parentheses give normalized ΔH values representing the CAB portion of the blend only

CAB fibres blended with 15 and 20 wt% L contents show small ($\sim 3\text{--}4\ \mu\text{m}$) pores in fibres with 15% L content and large pores ($\sim 7\text{--}10\ \mu\text{m}$) in fibres with 20% L content (Figures 4a and 4b). At 0% L, the fibre surface is relatively smooth with small pores ($\sim 1\text{--}3\ \mu\text{m}$). The increase in porosity with L content may be due to an increase in coagulation rate in the presence of L. The roughness of the fibre surface increases with increasing L content, but there are no indications of phase separation between CAB and L.

Transmission electron microscopy (TEM)

Further evidence of phase mixing between CAB and L is provided by TEM. Figures 5a and 5b show the skin and core of a single fibre cross-section, respectively, of CAB with 10% L content stained by RuO_4 . The maximum pore size (white regions) of the skin is $\sim 1\text{--}2\ \mu\text{m}$ and that of the core is less than $1\ \mu\text{m}$. This difference in skin and core morphology of the fibres is due to the solidification process during coagulation. The different pore sizes in the fibre cross-section are analogous to a foam structure. SEM and TEM results indicate that the size of the pores on the fibre surface increases with increasing L content. The total area of the pores in the core of all fibres was approximately 30%, as determined by digital imaging analysis. The continuous (dark) matrix represents the blended CAB/L morphology, and this implies considerable phase mixing. A similar morphology was observed for all the fibres with varying L content.

A single T_g was observed for all CAB/L fibres. This is as expected since both components have almost identical T_g values. It is also consistent with earlier work on films of CAB/L blends which also demonstrated single T_g transitions up to $\leq 20\%$ L content by d.s.c.¹⁵. While this alone does not provide sufficient evidence for phase miscibility, SEM and TEM results also fail to display signs of phase separation. This suggests that CAB/L fibres form a miscible amorphous phase. The improvement in the mechanical properties of CAB/L fibres can be attributed to high levels of mixing and the liquid crystalline order. It is expected that the lower viscosity, minor component (L) will disperse in the spinning

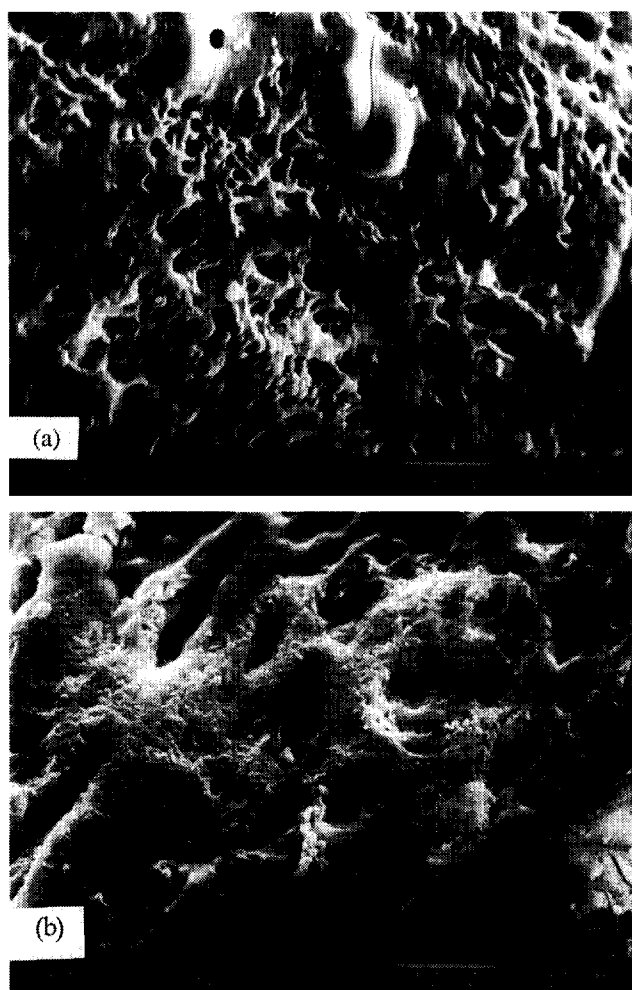


Figure 4 Scanning electron micrographs of the surface of CAB/L fibres with varying lignin content: (a) 15% L (w/w); and (b) 20% L (w/w)

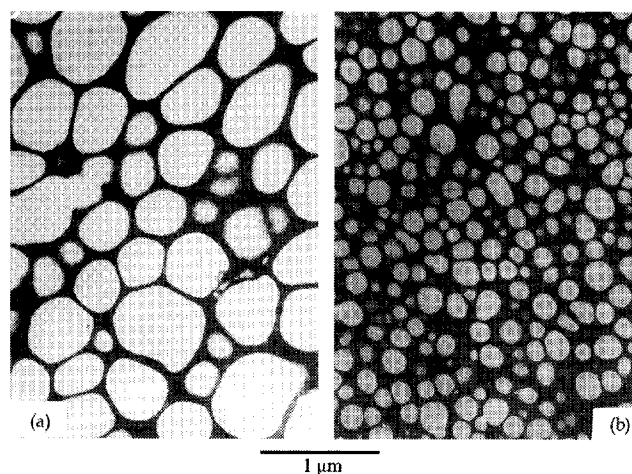


Figure 5 Transmission electron micrographs of the stained cross-sections of (a) skin and (b) core segment of CAB/L fibre containing 10% (w/w) lignin

solution and encapsulate the higher viscosity major component (CAB) during capillary flow²². Rearrangement and phase separation of the blend components with different viscosities is possible during spinning. Since such a rearrangement is a kinetic process, it usually does

not occur during wet spinning due to the immediate coagulation of the solution. This enhances the individual distribution of the blend components as shown in the CAB/L fibres. Fibre spinning is, therefore, a good route to producing blends with significant phase mixing.

CONCLUSIONS

1. Dynamic viscosity, dynamic elastic modulus and dynamic loss modulus all decrease with the lignin content of CAB/L blends.
2. Polarized optical microscopy results demonstrate that the blended solutions of CAB/L are liquid crystalline.
3. SEM and TEM provide evidence in support of fibre surface porosity, with pore size of CAB/L fibres increasing as L content decreases.
4. Modulus and tenacity of the fibres from CAB/L blends improve in the presence of L. This is attributed to the formation of mixed phases as observed by d.s.c., SEM and TEM. The high rate of coagulation during fibre spinning enhances phase mixing.

ACKNOWLEDGEMENTS

We appreciate the support of this research by the National Science Foundation Science and Technology Center for High Performance Polymeric Adhesives and Composites at Virginia Tech under contract DMR 8809714. Helpful counsel by Dr Garth L. Wilkes (Chemical Engineering) is acknowledged with gratitude.

REFERENCES

- 1 Walsh, D. J., Higgins, J. S. and Maconnachie, A. 'Polymer Blends and Mixtures', NATO ASI Series, Applied Sciences No. 89, Dordrecht, Martinus Nijhoff, 1985
- 2 Paul, D. R. and Newman, S. 'Polymer Blends', Vol. 1, Academic Press, New York, 1978
- 3 Olabisi, O., Robeson, L. M. and Shaw, T. M. 'Polymer-Polymer Miscibility', Academic Press, New York, 1979
- 4 Ophir, Z. and Ide, T. *Polym. Eng. Sci.* 1983, **23**(14), 792
- 5 Joseph, E., Wilkes, G. L. and Baird, D. G. *Polym. Eng. Sci.* 1985, **25**(7), 377
- 6 Suokas, E., Sarlin, J. and Tormala, P. *Mol. Cryst. Liq. Cryst.* 1987, **153**, 515
- 7 Pirnia, A. and Sung, C. S. P. *Macromolecules* 1988, **21**, 266
- 8 Hedmark, P. G., Lopez, J. M. R., Westdahl, M., Werner, P. -E., Jansson, J. -F. and Gedde, U. W. *Polym. Eng. Sci.* 1988, **28**(19), 1248
- 9 Flory, P. J. *Adv. Polym. Sci.* 1984, **59**, 1
- 10 Aharoni, S. M. *Polymer* 1980, **21**, 21
- 11 Bianchi, E., Ciferri, A. and Tealdi, A. *Macromolecules* 1982, **15**, 1268
- 12 Marsano, E., Bianchi, E. and Ciferri, A. *Macromolecules* 1984, **17**, 2886
- 13 Ambrosino, S., Khallala, T., Seurin, M. J., Ten Bosch, A., Fried, F., Maissa, P. and Sixou, P. *J. Polym. Sci., Polym. Lett.* 1987, **25**, 351
- 14 Rials, T. G. and Glasser, W. G. *J. Appl. Polym. Sci.* 1989, **37**, 2399
- 15 Rials, T. G. and Glasser, W. G. *Wood Fiber Sci.*, 1989, **21**(1), 80
- 16 Davé, V., Glasser, W. G. and Wilkes, G. L. *Polym. Bull.* 1992, **29**, 565
- 17 Davé, V., Glasser, W. G. and Wilkes, G. L. *J. Polym. Sci. Phys.* 1993, **31**, 1145
- 18 Davé, V. and Glasser, W. G. *J. Appl. Polym. Sci.* 1993, **48**, 683
- 19 Davé, V., Wang, J., Glasser, W. G. and Dillard, D. *J. Polym. Sci. Phys.* 1994, **32**, 1105
- 20 Davé, V. and Glasser, W. G., in 'Viscoelasticity of Biomaterials', ACS Symposium Series No. 489 (Eds W. G. Glasser and H. Hatakeyama), 1992, pp. 144-166
- 21 Hong, Y. K., Hawkinson, D. E., Kohout, E., Garrard, A., Fornes, R. E. and Gilbert, R. D., in 'Polymer Association Structures', ACS Symposium Series No. 384 (Ed. A. M. El-Nokaly), 1989, p. 184
- 22 Paul, D. R. in 'Polymer Blends', Vol. 2, Academic Press, New York, 1978, Ch. 16, p. 167